American Mineralogist, Volume 65, pages 1002–1011, 1980

Rapid-quench hydrothermal experiments in dilute chloride solutions applied to the muscovite–quartz–sanidine equilibrium

ROBERT P. WINTSCH, ENRIQUE MERINO AND ROBERT F. BLAKELY

Department of Geology, Indiana University
Bloomington, Indiana 47405

Abstract

We have conducted a series of experiments in 0.01-molal chloride solutions at 200°C and 2 kbar on the muscovite–quartz–sanidine equilibrium for variable solid/fluid ratios, which in these experiments are proportional to the surface area of the solids. The quench pH decreases with increasing solid/fluid ratios for runs with starting solution compositions in the sanidine field (*i.e.*, relatively alkaline solutions), but increases with increasing solid/fluid ratios for runs with starting solutions in the muscovite field (*i.e.*, relatively acid). The two trends intersect at a solid/fluid ratio of ~1/16, which is the ratio that yields the narrowest equilibrium reversals; in turn these reversals agree well with the independently-calculated log K (200°C, 2 kbar).

For the same reaction in 0.01-molal chloride solutions at 205°C and 17 bar vapor pressure, the same trend of quench pH-*vs.*-solid/fluid ratio is observed for the runs approaching equilibrium from the muscovite field as for the 2 kbar runs, but no clear trend emerges from the runs approaching equilibrium from the sanidine field. Taken together, the experiments at 2 kbar and 17 bar indicate that surface reactions cannot account for the two trends in quench pH; if they did, the trends observed on approaching equilibrium from both sides would be the same, which they are not. We conclude that dilute solutions are appropriate for collecting high-temperature/high-pressure equilibrium data provided one uses the rapid-quench technique with solid/fluid mass ratios of ~1/16.

The rapid-quench, dilute chloride solution technique was also used to determine log K *vs.* T for the muscovite–quartz–sanidine reaction at 2 kbar and solid/fluid ~1/16 over the interval 200–500°C. The log K's, determined *via* aqueous-speciation calculations for each T and P, coincide with the log K's calculated independently from the thermodynamic properties of the reactants and products.

Introduction

Experimental studies of solid–fluid equilibria have traditionally employed concentrated (1–2 molar) chloride solutions. Although these studies have generally been successful, the technique has several drawbacks. First, the amount of solid that must react in order to buffer the solution is relatively large, which increases the time necessary to establish equilibrium. Second, the use of concentrated chloride solutions causes activities of aqueous species to depart from the corresponding molalities and the activity of H_2O to depart from unity.[1] Both of these departures can alter the values obtained for the equilibrium constant of the reaction under investigation. The use of dilute solutions eliminates these problems, but introduces the uncertainty of interpreting quench pH because of the possible effect of surface reactions. In spite of the successful use of dilute chloride solutions in autoclave experiments (Usdowski and Barnes, 1972), no systematic study has yet been carried out of the possible distorting effects of surface reactions on quench pH. These effects might be more important in dilute than in concentrated solutions. We report the results of our experiments of reaction 1, along with an assessment of the rapid-quench pH technique in dilute chloride solution.

The reaction studied is:

$$3/2\text{K-feldspar} + H^+_{aq} \rightleftarrows 1/2\text{muscovite} + 3\text{quartz} + K^+_{aq} \qquad (1)$$

[1] The standard state adopted here for aqueous species is one of unit activity in a hypothetical one-molal solution referenced to infinite dilution at any temperature and pressure. The standard state chosen for H_2O and for minerals is one of pure liquid H_2O and pure solids, respectively, at any temperature and pressure.

0003–004X/80/0910–1002$02.00

For the standard states chosen here (see footnote 1), the equilibrium constant is

$$K_1 = a_{K^+}/a_{H^+} \quad (2)$$

This reaction was chosen because (1) it has been studied experimentally over a large range of temperature, pressure, and salinity (Hemley, 1959; Shade, 1968, 1974; Usdowski and Barnes, 1972; Gunter, 1974; Wintsch, 1975); (2) equilibrium constants may be calculated from the thermodynamic properties of the reactants and products (Helgeson and Kirkham, 1976; Helgeson *et al.,* 1978); (3) dissociation constants for the aqueous complexes of interest in the final solution are well known (Helgeson and Kirkham, 1976; Walther and Helgeson, 1977); and (4) the quench molalities of H^+ and K^+ may be easily measured with specific-ion electrodes (Usdowski and Barnes, 1972).

Many of our experiments have been designed to determine if surface reactions of the type discussed by Garrels and Howard (1959),

$$\text{K-mica} + H^+ = \text{H-mica} + K^+ \quad (3)$$

$$\text{K-feldspar} + H^+ = \text{H-feldspar} + K^+ \quad (4)$$

occur in rapid-quench experiments during the quench. Because these are surface reactions, the amount of hydrogen ion adsorbed will be proportional to the surface area of the minerals present. In order to vary the surface area in each experiment, the mass of the starting solids has been varied, keeping constant the mass of starting fluid. The particle size of the solids was always the same. Thus, the total mineral surface area is proportional to the mass of solids, and also to the solid/fluid ratio. Both high pressure and vapor pressure experiments have been carried out at 200°C for the purpose of contrasting the two different quenching techniques involved (see below).

Methods

Starting materials

Only synthetic quartz, muscovite and K-feldspar have been used in this study. They were prepared by using oxide mixes of reagent-grade H_2SiO_3, $AlCl_3 \cdot 6H_2O$, and K_2CO_3. The $AlCl_3 \cdot 6H_2O$ was heated at about 900°C for several hours to produce X-ray amorphous Al_2O_3. Appropriate mixtures of these materials were sealed in gold capsules with 0.05 g distilled–deionized H_2O, and starting materials were synthesized in standard cold-seal pressure vessels.

The grain size and unit-cell dimensions of the synthetic starting materials are listed in Table 1 along with the experimental conditions of synthesis. The X-ray technique suggested by Wright and Stewart (1968) using copper radiation ($\lambda Cu K\alpha_0 = 1.540562$Å) has been followed, except that U.S. Bureau of Standards silicon ($a = 5.43088$Å at 25°C) has been used as an internal standard instead of CaF_2 and that samples have been run at slower scanning rates (1/4° 2θ/min). Unit cell parameters were calculated from the measured 2θ values by the computer program of Burnham (1962). In all cases both 1M and $2M_1$ muscovite have been synthesized together, but intensity of 1M muscovite peaks is considerably larger than that of $2M_1$ muscovite. The relatively large errors in the refinements of the muscovite structures are a consequence of the overlapping 1M and $2M_1$ peaks. Synthetic K-feldspar is high sanidine with slightly anomalous cell dimensions. Unit-cell parameters for quartz are identical to those for α-quartz and are not included in Table 1. Aqueous chloride solutions of variable m_{KCl}/m_{HCl} ratios but constant chlorinity were prepared by mixing 10^{-2} molal KCl and 10^{-2} molal HCl solutions. All rapid-quench experiments were conducted in sealed gold capsules. A constant 0.30 g of solution was used in each run, and different amounts of muscovite + sanidine + quartz (always in the mass ratio of 1:1:1) were weighed as required to vary the mineral surface area.

High-pressure experiments

High-pressure experiments were carried out in rapid-quench cold-seal pressure vessels of the type figured by Rudert *et al.* (1976). The pressure and extension vessels were 30 and 25 cm long respectively. An 8-cm filler rod was used in each run to limit convection of the H_2O pressure medium. Temperatures were measured with sheathed chromel–alumel thermocouples standardized against the melting point of NaCl (800.5°C). Rudert *et al.* report temperature gradients in rapid-quench bombs which they believe are unacceptably large. We report our measured temperature gradients in some detail because so little is known about them and because our results are significantly smaller than those of Rudert *et al.*

Temperature gradients between the thermocouple well and the charge were determined by comparing the temperature measured in the thermocouple well with the melting temperature of tin (231.9°C), zinc (419.6), and antimony (630.7). These metals were sealed in evacuated silica tubes (5 to 6 cm long and 6 mm O.D.) of dimensions close to those of the gold

Table 1. Conditions of synthesis, grain size, and unit-cell dimensions of synthetic starting materials

Mineral	T°C	P(Kb)	Run duration (days)	Crystal dimensions (microns)	a (Å)	b (Å)	c (Å)	β (deg)	$\bar{V}$ (Å^3)	no. unique observations
San 3	520	2	14	30x30x40	8.6146 ±0.0060	13.0139 ± 0.0039	7.1699 ±0.0039	116.195 ± 0.033	721.26 ± 0.93	15
San 8	600	2	14	30x30x40	8.5877 ±0.0033	13.0116 ± 0.0029	7.1711 ±0.0022	116.101 ± 0.018	719.548 ± 0.485	16
Musc 12 (1M)	600	2	20	1x10x10	5.2036 ±0.0072	8.9822 ± 0.0029	10.2427 ±0.0053	101.710 ± 0.064	468.78 ± 0.73	13
Musc 12 ($2M_1$)	600	2	20	1x10x10	5.1787 ±0.0027	8.9840 ± 0.0019	20.1651 ±0.0056	95.865 ± 0.059	933.272 ± 0.66	16
Musc 14 (1M)	570	2	12	1x10x10	5.1984 ± .0089	8.9769 ± 0.0039	10.2504 ±0.0073	101.655 ± 0.085	468.47 ± 0.97	14
Musc 14 ($2M_1$)	570	2	12	1x10x10	5.1832 ±0.0039	8.9828 ± 0.0033	20.1779 ± .0105	95.620 ± 0.094	934.961 ± 0.96	12

capsules used. The amount of metal melted as a function of distance from the hot end could readily be measured by viewing the metal through the glass. Temperature gradients so measured are shown in Figure 1. They are smaller than those reported by Rudert *et al.*, particularly at higher temperatures.

The errors of precision, thermal gradient, and furnace temperature fluctuation combine to give an estimated temperature uncertainty of between 5 and 10°C. Pressures were monitored on a Heise 7kbar temperature-compensated pressure gauge. Because all bombs were isolated from line pressure during most of the run time, temperature fluctuations led to pressure fluctuations. The maximum pressure error this causes is ±50 bar.

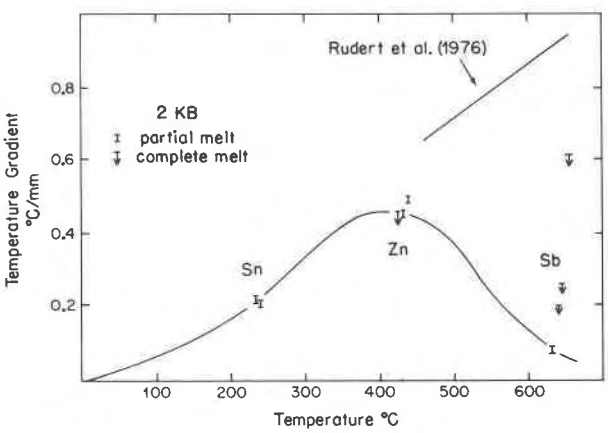

Fig. 1. The change in temperature gradient with temperature as determined by comparing the melting temperature of tin, zinc, and antimony (sealed in evacuated silica glass tubes) with the measured temperature in the thermocouple well. The data of Rudert *et al.* (1976) have been included for comparison. The temperature reported for each run is equal to the temperature given by the thermocouple minus a quantity which equals the temperature gradient (as given by this curve) multiplied by the distance between the thermocouple well and the gold reaction tube.

Vapor pressure experiments

In these experiments the sealed gold capsules were placed in a drying oven, and the temperature monitored with a thermocouple placed adjacent to the capsules on the same shelf in the oven. Pressure was the vapor pressure of the aqueous solution at the temperature of the experiment. Rapid quench was achieved by immersing the capsule in an ice bath.

Activity measurements

Both pH and pK of the final, quenched aqueous solutions were measured with specific-ion electrodes. A Beckman flat bulb combination pH electrode #39507 was used with a lithium trichloroacetate internal filling solution to prevent KCl contamination. The uncertainty in pH measurement is ±0.05. Orion's 93 series potassium-ion electrode was used in conjunction with the reference portion of the combination pH electrode to measure pK with an error of ±0.02. Orion digital pH meters were standardized to read KCl molality directly with the slope adjusted to 100%. Both electrodes were standardized before and after each experimental measurement.

All measurements were made in a glove box flushed with compressed air bubbled through NaOH solutions to remove CO_2 and through distilled water to ensure H_2O saturation. This process minimized CO_2 contamination and evaporation of the quenched solution during the measurement of activity. Approximately 4 minutes elapsed between the quench and insertion of the electrodes into the solution, and another ½ and 3 minutes were required to achieve

stable pK and pH readings respectively. The response of the pH electrode was monitored on a strip chart recorder, so that the rate of approach to a stable reading could be accurately assessed.

Run products

Following each experiment the silicates were examined by optical and X-ray techniques. The solutions were so dilute that very little new muscovite or sanidine precipitated during the experiment, and textural evidence was often insufficient to determine reaction direction. However, the growth of muscovite on sanidine crystals and the inclusion of muscovite and sanidine in quartz are taken as evidence of sanidine dissolution in solutions of low starting m_{KCl}/m_{HCl} ratio. Muscovite inclusions could be occasionally detected in sanidine crystals, indicating sanidine growth at the expense of muscovite + quartz. Euhedral quartz crystals about 10 × 50 microns crystallized in runs whose initial starting compositions were either in the muscovite or the sanidine field. In view of the irregular distribution of these textures, the direction of change in pH and pK provides a more reliable monitor of reaction direction and extent of reaction. X-ray scans of all run products have been made, but in no instance could a change in the polymorph of a phase be detected. In two runs, however, a peak at ~14Å was identified, and in both runs the amount of sanidine was much reduced.

Calculation of speciation

In order to obtain the ratio a_{K^+}/a_{H^+} (= K_{eq} for reaction 1) from the measured $m_{K,tot}$, the distribution of aqueous species must first be calculated for the aqueous solution from each run. We have calculated the speciation by solving the following nonlinear system of four mass-action-law equations (one each for the complexes KCl, HCl, KOH, and H_2O) and three mass balances (for K, H, and Cl):

$$m_{K^+}\,\gamma_{K^+}\,m_{Cl^-}\,\gamma_{Cl^-} = K_{KCl}\,m_{KCl^\circ}\,\gamma_{KCl} \quad (5)$$

$$m_{H^+}\,\gamma_{H^+}\,m_{Cl^-}\,\gamma_{Cl^-} = K_{HCl}\,m_{HCl^\circ}\,\gamma_{HCl} \quad (6)$$

$$m_{K^+}\,\gamma_{K^+}\,m_{OH^-}\,\gamma_{OH^-} = K_{KOH}\,m_{KOH^\circ}\,\gamma_{KOH} \quad (7)$$

$$m_{H^+}\,\gamma_{H^+}\,m_{OH^-}\,\gamma_{OH^-} = K_{H_2O}\,a_{H_2O} \quad (8)$$

$$m_{K,tot} = m_{K^+} + m_{KCl^\circ} + m_{KOH^\circ} \quad (9)$$

$$m_{Cl,tot} = m_{Cl^-} + m_{HCl^\circ} + m_{KCl^\circ} \quad (10)$$

$$m_{H,tot} = m_{H^+} + m_{HCl^\circ} \quad (11)$$

The seven unknowns are the molalities of K^+, H^+, OH^-, Cl^-, KCl°, HCl°, and KOH°. The activity of H_2O (see footnote 1) is a function (though a very insensitive one) of the molalities of those seven species, and it can be calculated by solving a system with the 7 equations above plus one similar to that of Wood (1975, eq. 14, p. 1150) which yields a_{H_2O} as a function of the molalities of individual aqueous species. (Wood's eq. 14 yields a_{H_2O} in terms of the stoichiometric molalities of neutral salts.) If we do this for all our runs a_{H_2O} comes out to be > 0.997, and therefore, to simplify matters, it has been set to 1.0 at any T, P.

In solving the system of equations we have calculated also (by iteration on the ionic strength) the individual-ion activity coefficients with the Stokes–Robinson equation modified by Helgeson (1969, eq. 43):

$$\log \gamma_i^*(T, P, \bar{I}) = \frac{-A(T, P) z_i^2 \bar{I}^{1/2}}{1 + \mathring{a}_i(T) B(T, P) \bar{I}^{1/2}} + \dot{B}(T)\bar{I} \quad (12)$$

and the activity coefficients for neutral complexes with the equation (Helgeson, 1969, eq. 36):

$$\log \gamma^\circ(T, \bar{I}) = \sigma \bar{I} \quad (13)$$

where γ_i^* and γ° are the individual activity coefficients; $\mathring{a}_i$ and z_i the distance of closest approach and charge for each species; A, B the Debye-Hückel coefficients; $\bar{I}$ the true ionic strength; and $\dot{B}$ and σ coefficients dependent on T. The temperature and pressure dependence of γ_i^* are incorporated in the coefficients A and B which were calculated from the dielectric constant and density of H_2O at the P, T of interest (Helgeson and Kirkham, 1974, their eqs. 2 and 3). Values for $\dot{B}$ at vapor pressure were taken from Helgeson (1969) without a pressure correction. Values of σ (eq. 13) up to 300°C were obtained from the data in Helgeson (1969, Table 2); for higher-temperature experiments, the 300°C value was used, and no pressure correction was made for the experiments at 2 kbar. Errors introduced by these approximations are very small. Note in particular that the quantities $\dot{B}\bar{I}$ and $\sigma\bar{I}$ in eqs. 12 and 13 are very small, insofar as $\dot{B}$ and σ are multiplied by true ionic strengths of less than $10^{-2}m$—another minor advantage of performing quench equilibrium experiments in dilute chloride solutions.

The input needed to solve the system of equations consists of four dissociation constants (taken for each T, P of interest from Helgeson and Kirkham, 1976, p. 110–111) and the total molalities for Cl, K, and H. Chloride was assumed unchanged from the starting molality, and the last two total molalities were measured directly in the quench solution at the end of each run. We have not made the assumptions of Montoya and Hemley (1975), who took the total con-

centrations of potassium in the initial and final solutions to be equal (which ignores take-up or release of potassium by the minerals), or of Shade (1968) and Usdowski and Barnes (1972), who took the activities of K^+ and Cl^- to be equal (which is probably inaccurate on account of the differences in molalities and activity coefficients for the two ions).

The actual solving was performed by the subroutine ZSYSTM (of the International Mathematical and Statistical Library), which requires a set of initial guesses for all the unknowns. The output for each solution consists of the molalities, activities, and activity coefficients for each species in the solution, the true ionic strength, and an echo of all the constants and initial guesses used. Four-significant-figure solutions were remarkably stable, never requiring more than six iterations.

Calculated equilibrium constants

Equilibrium constants for reaction 1 were calculated using the thermodynamic properties of the solids from Helgeson *et al.* (1978), and the partial molal volumes, heat capacity *T*, *P* functions, and entropies of ions from Helgeson and Kirkham (1976). The values obtained are shown in Figures 2, 3, 4 and 6. The calculations were performed with the computer program SUPCRT described by Helgeson *et al.* (1978, p. 202) and kindly provided by them. We do not know the error of these calculated equilibrium constants, but the effect of replacing the thermodynamic properties of sanidine by those of microcline in these calculations is shown in Figures 4 and 6.

Results

Initial and final experimental concentrations and calculated equilibrium constants for all experiments are given in Tables 2 and 3. Table 2 summarizes the experiments conducted at 205°C and 17 bar vapor pressure for a variety of solid/fluid ratios. Figure 2 illustrates the relationship between solid/fluid ratio and the calculated log (a_{K^+}/a_{H^+}) ratio for these experiments. Table 3 summarizes the results of experiments conducted at 2 kbar. Experiments 1 through 24 were run at temperatures near 200°C, 2 kbar, and at various solid/fluid ratios, and their relationship is shown in Figure 3. Experiments 25–32 were conducted at various temperatures at a solid/fluid ratio of 1/16 (see below), and are summarized in Figure 4.

Discussion

Effect of solid/fluid ratio

A variety of trends are established by the series of experiments in which the solid/fluid ratio is variable. Figures 2 and 3 show that log (a_{K^+}/a_{H^+}) increases with solid/fluid ratio, and thus with surface area, for experiments whose initial solution compositions were in the muscovite field (*i.e.*, relatively acidic). The data in Tables 2 and 3 show that these trends are caused primarily by increases in the pH in the runs, and that smaller increases in pK tend to lower the effect of pH on the activity ratio. For the experiments whose starting solution compositions were in the sanidine field (*i.e.*, were relatively alkaline), (a_{K^+}/a_{H^+}) decreases with increasing solid/fluid ratio at 2 kbar, but follows no clear trend at 17 bar (Figs. 2 and 3). The 2 kbar results are also shown in Figure 5 to depict the relationship between the calculated pH and pK as the solid/fluid ratio varies. For experiments approaching equilibrium from the muscovite field the pH and pK generally vary linearly with a slope of ~1 and an intercept of pH ~4.8. For runs in which

Table 2. Results of 45-day experiments at 205°C and 17 bar (vapor pressure), and calculated values of log (a_{K^+}/a_{H^+}), $\gamma_{K^+}/\gamma_{H^+}$, and ionic strength

run #	log solid/fluid	Initial pK	Initial pH	Initial log m_K/m_H	Final (Quench) pK	Final (Quench) pH	Final (Quench) log (m_{K^+}/m_{H^+})	Calculated log (a_{K^+}/a_{H^+})	Calculated $\gamma_{K^+}/\gamma_{H^+}$	Calculated $\frac{-1}{I} \times 10^4$
5	-2.72	2.00	4.05	2.05	2.05	5.70	3.65	3.60	0.975	87
6	-2.05	2.00	4.05	2.05	2.03	6.42	4.39	4.34	0.975	89
7	-0.99	2.00	4.05	2.05	1.96	6.22	4.26	4.21	0.973	96
8	-0.48	2.00	4.05	2.05	1.65	6.39	4.74	4.69	0.962	145
9	-2.60	2.00	9.21	7.21	2.05	5.96	3.91	3.86	0.975	87
10	-2.07	2.00	9.21	7.21	2.08	7.16	5.03	5.03	0.976	85
11	-1.00	2.00	9.21	7.21	1.97	6.15	4.18	4.13	0.973	94
12	-0.48	2.00	9.21	7.21	1.79	7.25	5.46	5.41	0.968	119
16	-1.75	2.00	10.02	8.02	1.92	5.57	3.65	3.60	0.972	100
17	-1.53	2.00	10.02	8.02	1.88	5.24	3.36	3.31	0.971	105

[1] *Molal units*

Table 3. Experimental results at 2 kbar total pressure, and calculated values of log (a_{K^+}/a_{H^+}), $\gamma_{K^+}/\gamma_{H^+}$, and ionic strength

run #	T°C	Run duration days	Log solid/fluid	Starting pK	Starting pH	Starting log (m_{K^+}/m_{H^+})	Final pK	Final pH	Final log (m_{K^+}/m_{H^+})	Calculated log (a_{K^+}/a_{H^+})	Calculated $(\gamma_{K^+}/\gamma_{H^+})$	Calculated $\bar{I}^5 \times 10^4$
1[1]	189 ± 5	55	-2.98	2.00	4.05	2.05	1.97	6.40	4.43	4.33	0.981	83
2	195 ± 2	55	-2.06	2.00	4.05	2.05	2.07	6.95	4.88	4.77	0.982	78
3	195 ± 2	55	-1.01	2.00	4.05	2.05	2.12	6.95	4.83	4.72	0.983	85
4	197 ± 3	55	-0.48	2.00	4.05	2.05	2.28	7.28	5.12	4.88	0.983	71
13	192 ± 3	42	-1.92	2.00	3.09	1.09	2.00	6.78	4.78	4.68	0.982	82
14	192 ± 3	42	-1.51	2.00	3.09	1.09	1.90	6.73	4.83	4.73	0.980	91
15	192 ± 4	45	-1.20	2.00	3.09	1.09	1.77	6.72	4.95	4.86	0.977	107
19[2]	200 ± 4	47	-2.67	2.00	10.02	8.02	2.00	8.46	6.46	6.33	0.965	179
20	209 ± 5	27	-1.92	2.00	10.02	8.02	2.00	7.51	5.51	5.40	0.979	91
21	199 ± 2	46	-1.58	2.00	10.02	8.02	1.98	7.60	5.62	5.51	0.979	94
22	201 ± 3	42	-1.31	2.00	10.02	8.02	1.82	7.08	5.26	5.16	0.977	102
23	203 ± 4	27	-0.96	2.00	9.75	7.75	1.72	6.46	4.74	4.65	0.975	114
24	201 ± 3	42	-0.48	2.00	10.02	8.02	1.38	5.28	3.90	3.83	0.960	209
25	262 ± 4	20	-1.22	2.00	3.08	1.08	1.89	6.48	4.59	4.47	0.976	90
26	362 ± 10	27	-1.20	2.00	3.24	1.24	1.72	6.58	4.80	4.67	0.968	96
27	476 ± 10	20	-1.24	2.00	3.08	1.08	1.92	5.96	4.04	3.87	0.969	63
28[3,4]	612 ± 4	20	-1.20	2.00	3.08	1.08	1.89	4.57	2.68	3.20	0.972	41
29	260 ± 6	20	-1.22	2.00	9.21	7.21	2.00	6.78	4.72	4.66	0.978	82
30	356 ± 3	20	-1.22	2.00	9.21	7.21	2.09	6.67	4.58	4.36	0.977	66
31	486 ± 2	20	-1.22	2.00	9.21	7.21	1.96	6.12	4.16	3.99	0.969	61
32[3]	623 ± 2	21	-1.24	2.00	9.21	7.21	1.94	4.61	2.67	3.20	0.974	38

[1] *No solid products present*
[2] *Too little solid products to allow x-ray analysis*
[3] *Solid products include a peak at 14 Å (= Al-montmorillonite?)*
[4] *No sanidine in run products*
[5] *Molal units*

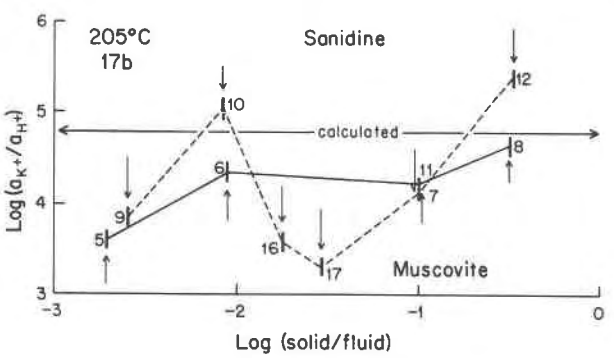

Fig. 2. Variation of log (a_{K^+}/a_{H^+}) with log (solid/fluid mass ratio) at 17 bar and 205°C. Each run is represented by a short vertical bar. The arrows show the direction of approach to equilibrium, and each number identifies a run in Table 2. Arrows pointing up and joined by the solid line refer to experiments in which the starting solution had a low a_{K^+}/a_{H^+} ratio, which is equivalent to saying that the solution was acid and that it was initially in the muscovite field. Arrows pointing down and joined by the dashed line refer to runs in which the starting solution had a high a_{K^+}/a_{H^+} (*i.e.*, a starting solution that was alkaline and in the sanidine field). The a_{K^+}/a_{H^+} for each run was calculated from quench measurements *via* the speciation of the final solution. The horizontal line at log $(a_{K^+}/a_{H^+}) \sim 4.8$ indicates the equilibrium constant for reaction 1 calculated from thermodynamic data in Helgeson *et al.* (1978) and Helgeson and Kirkham (1976).

equilibrium was approached from initially alkaline solutions a very steep trend is obtained in which the increase in a_{H^+} is much larger than that in a_{K^+}.

Surface reactions

Surface reactions like 3 and 4 could, in principle, affect the quench pH and produce the trends of Figures 3 and 4 if their exchange constants changed with temperature and pressure. However, these constants may either increase or decrease with temperature and thus only one trend at most could be explained by surface exchange. For example, if the exchange constants decreased, and especially if they become less than 1 at high P and T, these surfaces would begin to adsorb K^+ and desorb H^+. During the quench K^+ would be desorbed and H^+ adsorbed, causing m_{K^+}/m_{H^+} ratio to increase in the quench solution. This increase would be greater the greater the surface area, and could produce the trend established by the acid approach experiments of Figures 2 and 3. If, on the other hand, the exchange constants increased with increasing T and P, then the opposite pattern of surface exchange (*i.e.*, that obtained in the alkaline approach experiments, Fig. 3) would take place.

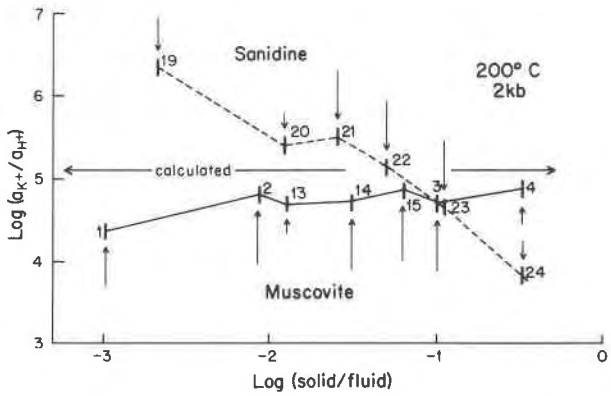

Fig. 3. Variation of log (a_{K^+}/a_{H^+}) *vs.* log (solid/fluid mass ratio) for reaction 1 at 200°C and 2 kbar total pressure. The horizontal line indicates the equilibrium constant for reaction 1 calculated from thermodynamic data—see caption to Fig. 2 for more details.

Which trend (if either) is more likely to be caused by surface reactions is determined by how and how much the exchange constants vary with changes in temperature and pressure. Considerations based on estimates of ΔS_r and ΔV_r for reactions 3 and 4 point to increasing exchange equilibrium constants, K_{ex}, with increasing temperature, and therefore only the trend of decreasing m_{K^+}/m_{H^+} with increasing solid/fluid (Fig. 3) could, in principle, be explained by surface adsorption. The experimental results of Dugger *et al.* (1964) for the surface exchange gel–SiOK + H^+_{aq} = gel–SiOH + K^+_{aq} tend to confirm the above prediction of increasing K_{ex} with increasing T. Actual values for K_{ex} of reactions 3 and 4 are only available at low temperatures. At 25°C and 1 bar, $K_3 = 10^{7.4}$ and $K_4 = 10^{9.5}$ (Garrels and Howard, 1959). The only high T–P data bearing on the problem are those of Currie (1968), who measured the solubility of albite in pure H_2O at 400–600°C and 0.75–3.5 kbar. He showed that Na/Al in the experimental solutions was always higher than in albite, and that the pH of the final solutions varied between 9.64 and 10.63, depending on the experimental conditions. The high Na^+_{aq} and low H^+_{aq} content of the experimental solutions imply that at these large temperature–pressure conditions H^+ was strongly preferred to Na^+ on the feldspar surface. Hydrolysis of ions released by congruent dissolution of the albite also changes the pH, but not by several pH units, as in Currie's experiments. Thus all the experimental evidence, though scant, suggests that these silicate surfaces strongly prefer H^+ to K^+ (or Na^+) over a wide range of temperatures and pressures.

Given, therefore, that the K_{ex}'s for surface exchange reactions 3 and 4 are $\gg 1$ at both low and high temperatures, how much would surface exchange reactions change the m_{H^+} upon quench? Order-of-magnitude calculations of such an effect yield changes in the m_{H^+} in solution of $\sim 10^{-13}$ moles/liter for the lowest solid/fluid ratio and $\sim 10^{-10}$ moles/liter for the highest solid/fluid ratio, even allowing the high-temperature K_{ex} to increase or decrease by three orders of magnitude with respect to its value at low temperature. [The calculations involved averages of particle size and surface charge density, the actual masses of the solids and fluid in our experiments (Tables 2 and 3), and the actual experimental water compositions.] Because these quantities (10^{-13}–10^{-10} mole H^+/liter) are so much smaller than the actual pH changes measured (up to three pH units, see alkaline trend, Fig. 3), it can safely be concluded that neither of the quench pH trends of Figure 3, not even the trend established by the alkaline approach experiments, can result from the surface reactions.

Approach to equilibrium

The approach of these experiments to equilibrium can only be assessed by the degree of approach of

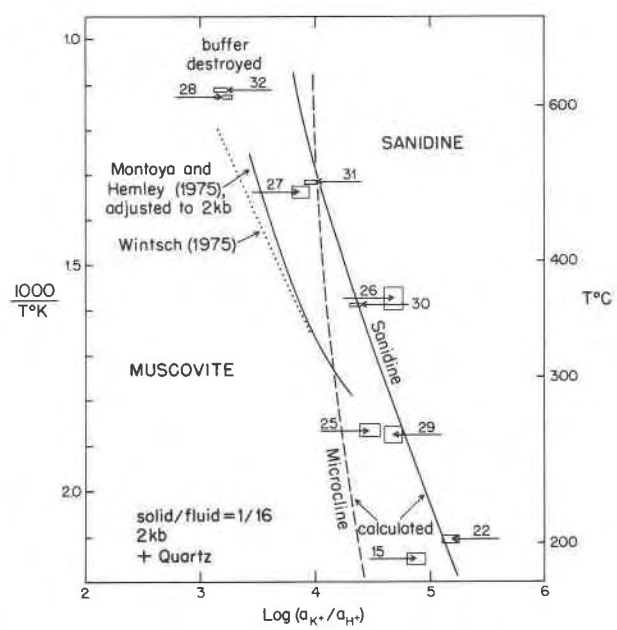

Fig. 4. The variation with temperature of the log (a_{K^+}/a_{H^+}) calculated (*via* the speciation) from experiments conducted at 2 kbar in 10^{-2} molal Cl^- solutions at a solid/fluid ratio of 1/16. Boxes give uncertainty limits, and arrows indicate the direction of approach to equilibrium (see caption to Fig. 2). The solid curve was independently calculated from thermodynamic data for minerals and aqueous species in Helgeson *et al.* (1978), Helgeson and Kirkham (1976), and Walther and Helgeson (1977).

a_{K^+}/a_{H^+} ratios at similar solid/fluid ratios. The systematic trends of Figure 3 show that the closest approach to equilibrium of initially very different starting solutions is obtained at a solid/fluid ratio of $\sim 10^{-1.2} = 1/16$. The experiments at 17 bar (Fig. 2) suggest an optimum solid/fluid ratio of ~1/10, but because they are more erratic than those at 2 kbar, 1/16 appears to be the most favorable solid/fluid ratio to approach equilibrium most closely.

Higher-temperature experiments

Experiments investigating reaction 1 have been conducted at ~260, 360, 480, and 620°C at 2 kbar, and at a solid/fluid ratio of 1/16. Figure 4 shows that all experiments between 200° and 500°C except #26 form tight reversals of reaction 1. Comparison of these reversals with the calculated equilibrium constant *vs.* temperature curve shows good agreement between the two. Two experiments (28 and 32) above 600°C on Figure 4 fall to the left of the calculated line but very close to each other. In each case a 14Å phase (aluminum montmorillonite?) was produced, destroying the buffer assemblage of reaction 1. Thus these two points should not plot with the lower-temperature results because a different assemblage buffers these experiments. These two experiments are nevertheless compatible with what is known about this chemical and mineralogical system, because all theoretically calculated equilibrium constants for muscovite–aluminosilicate lie to the left of the muscovite–sanidine line. The convergence of the solution compositions of these two runs suggests that a close approach to (probably metastable) equilibrium has been achieved. Thus these 600°C results further support the reliability of the rapid-quench technique, because they yield solution compositions in general agreement with theoretical prediction and because they are closely reversed.

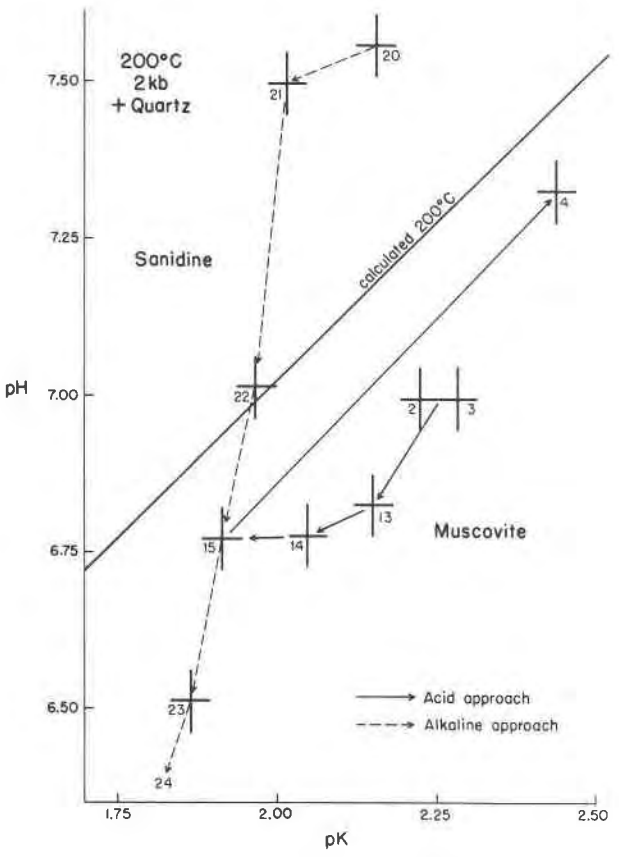

Fig. 5. Calculated ($-\log a_{H^+}$) *vs.* calculated ($-\log a_{K^+}$) for experiments conducted near 200°C at 2 kbar. The crosses indicate the uncertainties in the activities. The equilibrium constant calculated from thermodynamic data for minerals and aqueous species at 200°C is given by the slope of the solid line. See caption to Fig. 2 for more details.

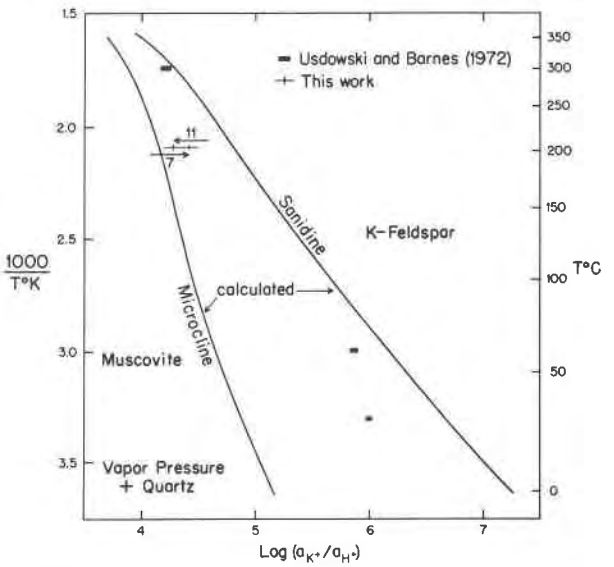

Fig. 6. The variation with temperature of the log (a_{K^+}/a_{H^+}) calculated from experiments of this study and from Usdowski and Barnes (1972). The equilibrium constants calculated theoretically for reaction 1 using alternatively microcline and sanidine are included for comparison.

Comparison with other work

Our results at 200°C and 17 bar are compared in Figure 6 to the work of Usdowski and Barnes (1972) and to the calculated equilibrium constants for microcline and sanidine. In view of the different experimental techniques and starting materials used in these two experimental studies, the results are in re-

markable agreement with each other. Also, the experimental data are in reasonable agreement with the calculated curves.

Higher-pressure experiments have been conducted on reaction 1 by Hemley (1959), Shade (1968, 1974), Gunter (1974), and Wintsch (1975). Most of these results are difficult to compare with the present study because the experiments were conducted at different pressures or chlorinities from those reported here. The study of Wintsch (1975) includes five experiments run at 2 kbar in 10^{-2} molal solutions. This curve lies at activity ratios approximately 0.4 log units smaller than the results reported here. These experiments involved solid/fluid ratios of between 1/30 and 1/60, and the data in Table 3 show that half of the discrepancy between the two experimental studies could be a consequence of this smaller solid/fluid ratio. The error in the activity ratio of these experiments is ±0.2 log units. Thus within the uncertainty of the data, the results of this study and of Wintsch (1975) are in agreement.

It is difficult to compare the calculated activity ratios of Shade (1968, 1974) and Montoya and Hemley (1975) with our calculations, because the former studies do not include the computation of activity coefficients, the calculations of Shade (1968, 1974) involve the simplifying assumption that $a_{K^+} = a_{Cl^-}$, which is not strictly valid, and the calculations of Montoya and Hemley (1975) are for 1 kbar. We have, however, adjusted the activity ratios of Montoya and Hemley to 2 kbar. The corrected ratios are included in Figure 4 for comparison. In view of the different methods involved in these calculations, they are in reasonable agreement.

The data in Figure 4 are thus significant because the equilibrium constant for reaction 1 at 2 kbar as a function of temperature has been obtained by a variety of methods that yield similar results. Within the limits of the errors involved, the equilibrium constants calculated from Hemley's (1959) experiments at 1 kbar in 2-molar solutions are indistinguishable from those calculated in this study from experiments at 2 kbar in 10^{-2} molal solutions. Both of these results agree with the equilibrium constants calculated from the thermodynamic data of Helgeson *et al.* (1978) which were, in turn, calculated from other experimental studies involving the synthetic minerals of reaction 1. We conclude, therefore, that the thermodynamic properties of synthetic muscovite, sanidine, and quartz are uniform from laboratory to laboratory.

Conclusions

From the data summarized in Figures 2 and 3 it appears that surface reactions do not affect quench pH in dilute solutions. Although we have no explanation for the observed trends of pK and pH *vs.* the solid/fluid ratio, they suggest that the narrowest reversals are obtained at solid/fluid ratios of 1/16. Significantly, these narrowest reversals are also the ones closest to the calculated log K.

We recommend that the aqueous concentrations of all elements be measured after quench for two reasons: to better monitor the approach to equilibrium of the solutions with the whole assemblage, and to allow for a more thorough calculation of the speciation of the final solution (in this case the addition of silica and aluminum species).

The agreement of our equilibrium constants, determined from experiments in dilute solutions, with the constants determined by others from experiments in concentrated solutions, and with constants calculated from an internally-consistent set of thermodynamic properties is remarkable. Clearly, accurate high-temperature/high-pressure solid–fluid equilibrium data can be obtained from experiments involving dilute chloride solutions.

Acknowledgments

It is a pleasure to thank H. C. Helgeson and G. C. Flowers of the University of California at Berkeley for their prompt and enlightening answers to many queries and for the computer program SUPCRT. We also thank E. Inouye, C. Moore, and B. Ransom for assistance in the laboratory, W. Moran and B. Moore for drafting, and T. F. Brown and S. Douthitt for typing. We acknowledge the support of the National Science Foundation (grant EAR 76-22560), of the Indiana University Foundation, and of the Indiana Geological Survey. The IMSL subroutines are a proprietary package of the International and Statistical Libraries. We acknowledge computer time given by Indiana University's Wrubel Computing Center, which also obtained the routines.

References

Burnham, C. W. (1962) Lattice constant refinement. *Carnegie Inst. Wash. Year Book, 61,* 132–135.

Currie, K. L. (1968) On the solubility of albite in supercritical water in the range 400 to 600°C and 750 to 3500 bars. *Am. J. Sci., 266,* 321–341.

Dugger, D. L., J. H. Stanton, B. N. Irby, B. L. McConnell, W. W. Cummings and R. W. Maatman (1964) The exchange of twenty metal ions with the weakly acidic silanol group of silica gel. *J. Phys. Chem., 68,* 757–760.

Garrels, R. M. and P. Howard (1959) Reactions of feldspar and mica with water at low temperature and pressure. In A. Swineford, Ed., *Clays and Clay Minerals,* p. 68–88. Pergamon Press, New York.

Gunter, W. D. (1974) *An experimental study of mineral-solution*

equilibria applicable to metamorphic rocks. Ph.D. Thesis, The Johns Hopkins University, Baltimore, Maryland.

Helgeson, H. C. (1969) Thermodynamics of hydrothermal systems at elevated temperatures and pressures. *Am. J. Sci., 267,* 729–804.

——— and D. H. Kirkham (1974) Theoretical prediction of the thermodynamic behavior of aqueous electrolytes at high pressures and temperatures: II. Debye-Hückel parameters for activity coefficients and relative partial molal properties. *Am. J. Sci., 274,* 1199–1261.

——— and ——— (1976) Theoretical prediction of the thermodynamic behavior of aqueous electrolytes at high pressures and temperatures: III. Equation of state for aqueous species at infinite dilution. *Am. J. Sci., 276,* 97–240.

———, J. M. Delany, H. W. Nesbitt and D. K. Bird (1978) Summary and critique of the thermodynamic properties of rock-forming minerals. *Am. J. Sci., 278-A,* 1–229.

Hemley, J. J. (1959) Some mineralogical equilibria in the system K_2O–Al_2O_3–SiO_2H_2O. *Am. J. Sci., 257,* 241–270.

Montoya, J. W. and J. J. Hemley (1975) Activity relations and stabilities in alkali feldspar and mica alteration reactions. *Econ. Geol., 70,* 577–583.

Rudert, V., I-M. Chou and H. P. Eugster (1976) Temperature gradients in rapid-quench cold-seal pressure vessels. *Am. Mineral., 61,* 1012–1015.

Shade, J. W. (1968) *Hydrolysis Equilibria in the System K_2O-Al_2O_3-SiO_2-H_2O.* Ph.D. Thesis, The Pennsylvania State University, University Park, Pennsylvania.

——— (1974) Hydrolysis reactions in the SiO_2-excess portion of the system K_2O–Al_2O_3–SiO_2–H_2O in chloride fluids at magmatic conditions. *Econ. Geol., 69,* 218–228.

Usdowski, H. E. and H. L. Barnes (1972) Untersuchungen über das Gleichgewicht zwischen K-Feldspat, Quarz und Muskovit und die Anwendung auf Fragen der Gesteinsbildung bei tieferen Temperaturen. *Contrib. Mineral. Petrol., 36,* 207–219.

Walther, J. V. and H. C. Helgeson (1977) Calculation of the thermodynamic properties of aqueous silica and the solubility of quartz and its polymorphs at high pressures and temperatures. *Am. J. Sci., 277,* 1315–1351.

Wintsch, R. P. (1975) Muscovite, sanidine, sillimanite, quartz and H_2O equilibria as a function of chloride concentration (abstr.). *EOS, 56,* 465–466.

Wood, J. R. (1975) Thermodynamics of brine–salt equilibria—I. The systems NaCl–KCl–$MgCl_2$–$CaCl_2$–H_2O and NaCl–$MgSO_4H_2O$ at 25°C. *Geochim. Cosmochim. Acta, 39,* 1147–1163.

Wright, T. L. and D. B. Stewart (1968) X-ray and optical study of alkali feldspar. I. Determination of composition and structural state from refined unit-cell parameters and 2*V*. *Am. Mineral., 53,* 38–87.

Manuscript received, September 17, 1979;
accepted for publication, January 30, 1980.